Journal of the Physical Society of Japan
Vol. 71, No. 2, February, 2002, pp. 543–549

Transport in Two-Dimensional Electron Gas with Isolated Magnetic Barriers

Masahiro HARA[1*], Akira ENDO[1], Shingo KATSUMOTO[1,2] and Yasuhiro IYE[1,2]

[1]*Institute for Solid State Physics, University of Tokyo, 5-1-5 Kashiwanoha, Kashiwa, Chiba 277-8581*
[2]*CREST Project, Japan Science and Technology Corporation, 1-4-25 Mejiro, Toshima-ku, Tokyo 171-0031*

(Received July 16, 2001)

We have studied the transport in two-dimensional electron gas (2DEG) subjected to two different types of magnetic barriers—dipolar and monopolar barriers—using fringing magnetic field from ferromagnetic film on the surface of GaAs/AlGaAs heterostructures. Resistivity of 2DEG increases as the magnetic barriers are turned on. We measured amplitude dependence and temperature dependence of the excess resistivities due to those magnetic barriers. The resistance as a function of the uniform component of the magnetic field exhibits a positive magnetoresistance and a beating pattern of the Shubnikov-de Haas oscillations. They are qualitatively explained by considering the various cyclotron trajectories in the region of the magnetic barriers.

KEYWORDS: GaAs/AlGaAs, 2DEG, magnetic barrier, electron-electron scattering, positive magnetoresistance, Shubnikov–de Haas oscillations
DOI: 10.1143/JPSJ.71.543

1. Introduction

Electron transport in laterally modulated two-dimensional electron gas (2DEG) has been investigated extensively in recent years. Weiss *et al.*[1)] generated 1D periodic weak electric potential by interference of laser beams, and observed a novel type of magnetoresistance oscillation, so-called Weiss oscillation. The phenomenon is interpreted as guiding-center drift resonance effect arising from commensurability between the cyclotron diameter and the electrostatic modulation period.[2)] The magnetoresistance ρ_{xx} takes minima at

$$\frac{2R_c}{a} = n - \frac{1}{4} \quad (n = 1, 2, 3, \cdots). \tag{1}$$

Here R_c is the cyclotron radius and a is the modulation period which is typically several hundred nanometer. It was predicted by a few authors[3–5)] that similar oscillatory magnetoresistance should be found for periodic magnetic field modulation. For 1D periodic magnetic modulation, the expected positions of ρ_{xx} minima are given by

$$\frac{2R_c}{a} = n + \frac{1}{4} \quad (n = 1, 2, 3, \cdots). \tag{2}$$

The initial attempt by Yagi and Iye[3)] to observe this magnetic Weiss oscillation was hampered by the dominance of strain-induced electrostatic potential modulation. Later, a few groups[6–8)] succeeded in observing the magnetic Weiss oscillation by circumventing the strain-induced effect in different ways.

Another topic of interest in periodically modulated systems is the excess resistance i.e., resistance increase due to the modulation potential, or lateral superlattice. Messica *et al.*[9)] found that the low temperature resistivity of a 2DEG subjected to a one-dimensional electrostatic potential modulation changes from the phonon-limited T-linear behavior to T-quadratic behavior as the modulation amplitude is increased. A T-quadratic resistivity was also observed in the magnetic modulation case.[10,11)] The T-quadratic excess resistivity is attributed to electron-electron Umklapp scattering process in the system where continuous translational symmetry is broken artificially. Recently, Kubrak *et al.* have investigated the excess resistance due to a single magnetic barrier.[12)] In this work, we investigate the transport through isolated magnetic barriers. We compare our results with the previous studies on similar systems,[12)] and with the case of periodic modulation.[10,11)]

2. Experimental

Our samples were fabricated from a GaAs/AlGaAs single-heterojunction wafer grown by molecular beam epitaxy. The electron density and mobility of the 2DEG at 4.2 K were 3.0×10^{15} m^{-2} and 40 m^2/Vs, respectively. The depth of the 2DEG plane from the sample surface was 75 nm. An array of cobalt strips was deposited on top of the current arm of a standard Hall-bar. The width of the Hall bar is 30 μm, and the separation between the voltage probes is 60 μm. The strain-induced electrostatic potential between the ferromagnetic strips and the heterostructure can be minimize by patterning the Hall-bar with the current direction along the non-piezoelectric [100] direction.[13)]

The transport measurements were carried out using a low-frequency ac technique. A cross-coil superconducting magnet system used in the present study consisted of a 6 T split-coil magnet and a homemade 1 T solenoid. It enabled us to control the horizontal and vertical components of the magnetic field independently. The ferromagnetic strips were fully magnetized by applying a strong enough magnetic field (5 T) parallel to the 2DEG plane. To a first approximation, the parallel magnetic field does not affect the orbital motion of the 2D electrons.

Two different types of magnetic barrier were made. Schematic diagrams of sample configuration are shown in Fig. 1. One type, ''dipolar magnetic barrier'' which consists of a pair of tightly-spaced positive and negative local magnetic field is created by the fringing field generated by a narrow ferromagnetic wire magnetized perpendicularly to its long side [Fig. 1(a)]. The other, ''monopolar magnetic barrier'' which is a local magnetic peak of either sign is generated at the edge of a wide ferromagnetic film [Fig. 1(b)]. In the actual samples, many such barriers were placed with the mutual separation comparable to or greater than the

*E-mail: hara@issp.u-tokyo.ac.jp

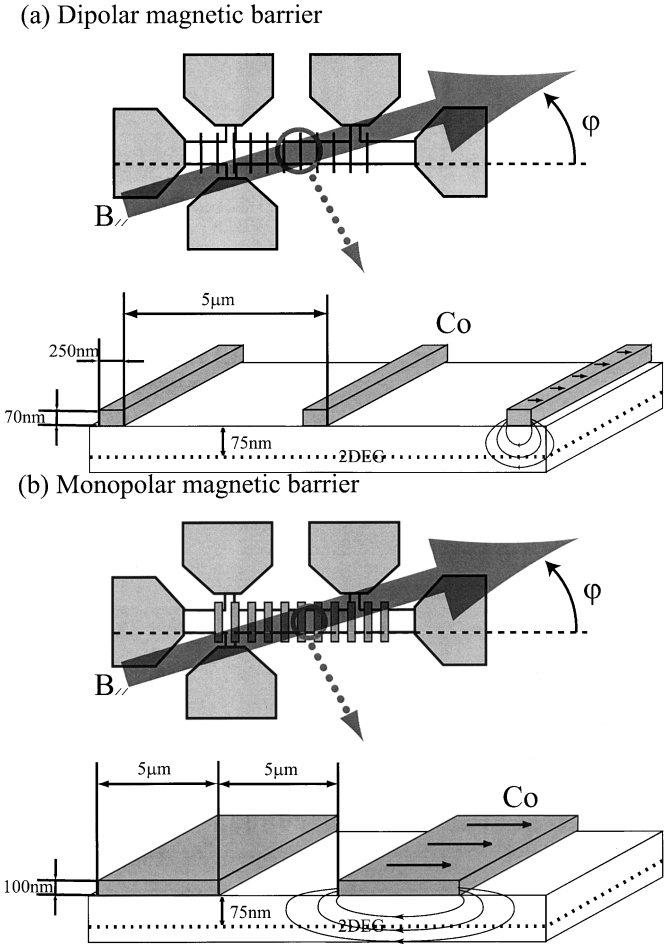

Fig. 1. Schematic diagram of sample configuration. (a) Dipolar magnetic barriers. (b) Monopolar magnetic barriers. Amplitude of the magnetic barrier was controlled by changing the azimuthal angle φ of the horizontal field.

electron mean free path. Transmission of electron through each magnetic barrier is ballistic, but momentum relaxation occurs between the barriers so that each magnetic barrier can be treated independently. When the separation between the dipolar barriers is made much smaller than the mean free path, the system is reduced to the periodic modulation case we studied earlier.[10,11]

The amplitude of the fringing field was precisely controlled by changing the azimuthal angle φ of the horizontal field with respect to the ferromagnetic strips.[10] The peak value of the local magnetic field B_0 could be varied as $B_0 = B_0^{\max}\cos\varphi$, where $B_0^{\max}$ denotes the maximum amplitude (typically a few hundred mT), which depended on the material and the thickness of the ferromagnetic film and on the depth of the 2DEG plane. We have calculated magnetic field profile for the two types of barrier by integrating magnetic moment assuming that the magnetization of ferromagnetic strips is fully saturated in the direction of the applied magnetic field. Figure 2 shows the normal component of the fringing magnetic field $B_z(x)$ and the corresponding vector potential $A_y(x)$ in the case that the horizontal magnetic field is parallel to the current direction ($\varphi = 0^\circ$). We were able to independently sweep the uniform perpendicular magnetic field while keeping the strength of the magnetic barriers constant to measure the magnetoresistance in the presence of magnetic barriers.

3. Amplitude Dependence

In this and next section, we discuss the excess resistivity due to the magnetic barriers in the absence of the uniform component of magnetic field. The resistivity of the 2DEG increases as the magnetic barriers are turned on. We investigated the dependence of the excess resistivity on the amplitude of the magnetic barrier B_0 which changes as $B_0 = B_0^{\max}\cos\varphi$. Figure 3 shows the excess resistivities as a function of $\cos\varphi$. In the case of the dipolar barriers, $\Delta\rho$ is proportional to $B_0^{3/2}$. This is similar to what we found for the case of periodic magnetic field modulation.[14] The $B_0^{3/2}$-dependence is in accordance with the theoretical prediction by Matulis and Peeters,[15] who consider the semiclassical electron trajectories in the presence of the magnetic barriers. They calculate the critical angle ϕ_c of the incident electron wave vector which separates whether a particular trajectory transmits through or is reflected from the magnetic barrier. The resistance change due to the magnetic barrier is obtained by considering that the reflected electron cannot make a contribution to the conductance. In the case of the periodic magnetic field modulation, similar consideration divides the semiclassical trajectories into propagating orbits and snake orbits, the latter being bounded in the x-direction. In both cases, i.e., periodic magnetic modulation and single magnetic barriers, it is predicted that the excess resistivity varies as $\Delta\rho \sim B_0^{3/2}$ for small values of B_0. However, for the monopolar barriers, we found somewhat stronger dependence $\Delta\rho \sim B_0^{\nu}$ with $\nu \sim 1.8$. Similar observation has been reported by Kubrak *et al.*, who found $\Delta\rho \sim B_0^{3/2}$ for dipolar barriers and $\Delta\rho \sim B_0^2$ for monopolar barriers.[12] Although the origin of the stronger dependence is not clear at the moment, the following two points may be relevant.

First, as seen in Fig. 2 the peak value of local magnetic field is larger for the monopolar barrier than the dipolar one. In the semiclassical theory,[15] it should be recalled that the $B_0^{3/2}$-dependence is obtained by assuming smallness of B_0. If the amplitude of the magnetic barrier is large enough that any trajectory is reflected from the barrier, the resistivity is infinite in the collisionless limit. So, the power ν is expected to become stronger as B_0 is increased.

Second, the dipolar and monopolar magnetic barriers differ in the deflection of transmitted electrons. The direction of the velocity vector $\boldsymbol{v}$ of an electron after it has passed through a dipolar barrier is the same as the initial one. By contrast, the velocity vector is always deflected by a monopolar barrier.

To make the first point more explicit, let us consider the deflection of electrons by magnetic barriers in some details. Electron motion in 2DEG under a spatially varying magnetic field is described by the following Hamiltonian.

$$H = \frac{1}{2m}p_x^2 + \frac{1}{2m}\left(p_y + eA_y(x)\right)^2 \tag{3}$$

The vector potential $A_y(x)$ for the two types of magnetic barriers are shown in Fig. 2. Here the spatial variation is only along the x-direction, so that the momentum p_y is conserved. In phase space (x, p_x, p_y), electron moves along the trajectory defined by the intersection of the Fermi surface with the $p_y = C$ plane (Fig. 4). Critical angle ϕ_c which

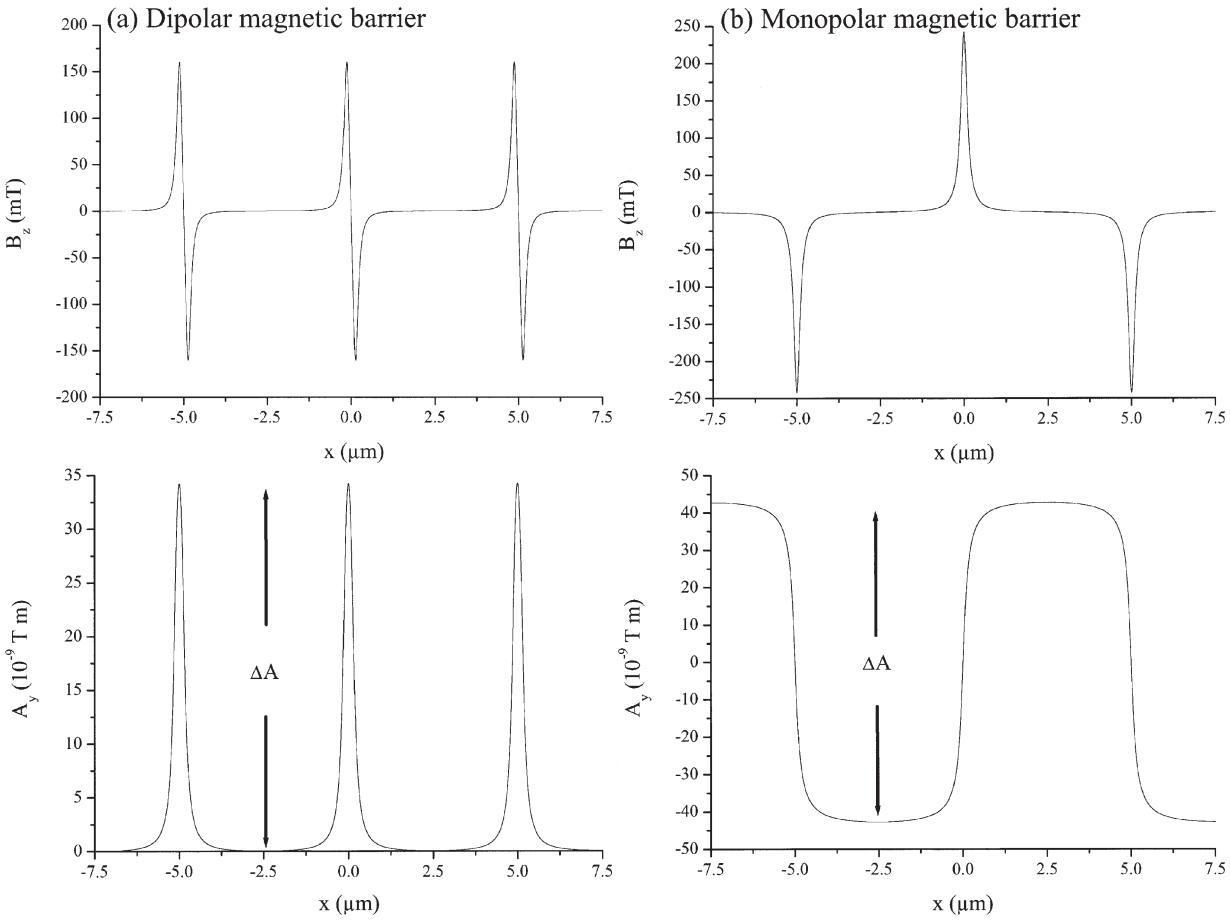

Fig. 2. Calculated magnetic field profile $B_z(x)$ and vector potential $A_y(x)$ ($\varphi = 0°$: maximum value) of two different magnetic barriers. Saturation of magnetization for cobalt is assumed to be 1.8 T.

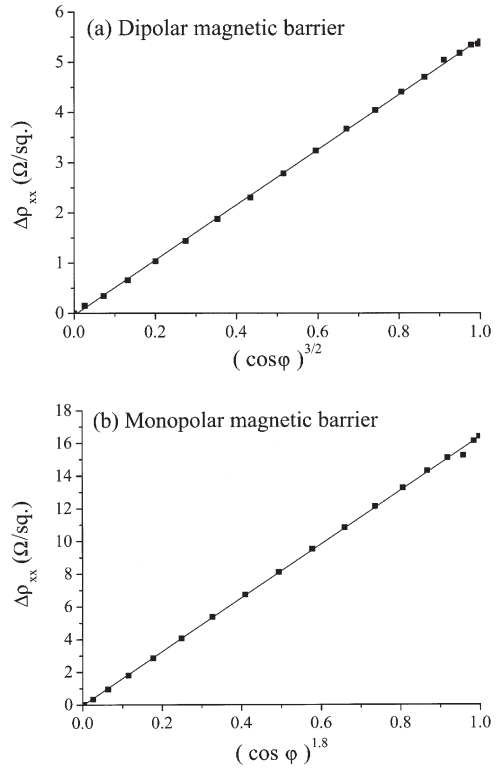

Fig. 3. Amplitude dependence of excess resistivity. Amplitude of magnetic barrier was changed linearly to $\cos\varphi$.

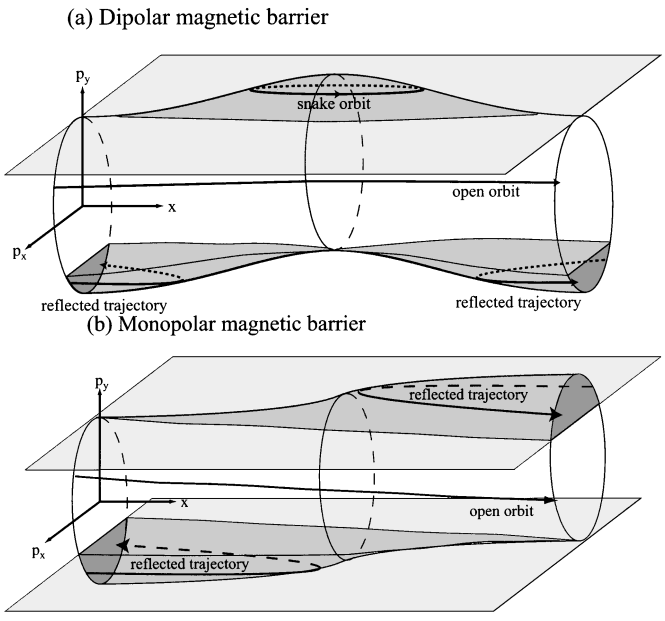

Fig. 4. Fermi surface around magnetic barrier in phase space (x, p_x, p_y).

separates whether electron transmits through or is reflected from the magnetic barrier is given by

$$\phi_c = \arccos\left(1 - \frac{e\Delta A}{\hbar k_F}\right) \tag{4}$$

$$\Delta A = \max\{A_y(x)\} - \min\{A_y(x)\} \tag{5}$$

According to the estimation of the vector potential $A_y(x)$ (Fig. 2),

$$\frac{e\Delta A}{\hbar k_F} \approx \begin{cases} 0.38 \text{ (Dipolar)} \\ 0.99 \text{ (Monopolar)} \end{cases} \tag{6}$$

The actual magnetic modulation may be smaller than the estimation, but the monopolar barrier sample obviously does not satisfy the assumption $e\Delta A/\hbar k_F \ll 1$. From the data for smaller values of $\cos\varphi$ alone, it is difficult to uniquely determine the power ν.

4. Temperature Dependence

Let us now turn to the temperature dependence of the excess resistivity. In the context of the model by Matulis and Peeters,[15] thermal fluctuation tends to suppress the excess resistance caused by the magnetic barriers. Experimentally, however, $\Delta\rho$ is found to increase with temperature as $\Delta\rho \sim AT^2 + C$ at $T \leq 15\,\mathrm{K}$ (Fig. 5). Such quadratic temperature dependences have been commonly observed for the both types of magnetic barriers and also for the periodic modulation case.[10,11] In this respect, Kubrak *et al.*[12] report different results. For the dipolar barrier they found the excess resistance to increase in proportion to the total resistance and hence was linear in T at low temperatures. For the monopolar barrier, they found no temperature dependence. However, their data points are rather sparse for detailed discussion of the temperature dependence.

In our earlier publications,[10,16,17] we interpreted the phenomenon in terms of electron–electron Umklapp process activated by the artificial superperiodicity. Recently, Uryu and Ando[19] have developed a theory considering electron–electron Umklapp scattering for the case in which the two-dimensional electron system is clean enough to form minigaps due to weak periodic potential. In the present study, the temperature-quadratic behavior of excess resistivity has been observed not only in the periodically modulated systems, but also for isolated magnetic barriers. This suggests that the periodicity of modulation *per se* is not essential in the phenomenon. However, we should mention that the T^2-term originates from electron–electron scattering, which we have shown in the experiment of the warm electron effect.[16] In this context, it is noteworthy that Sasaki and Fukuyama propose a novel T^2-term due to electron-electron scattering in periodically modulated systems which originates not from Umklapp process but from normal momentum conserving process.[18] When electron-electron scattering occurred under spatially varying magnetic field, total momentum of scattering electrons is conserved, but not the current. This theory also applies to the case of the isolated magnetic barriers.

Possible reasons for the deviation from the T^2-dependence at higher temperatures are discussed in ref. 10 for the periodic case. At higher temperatures, a few sources of corrections to the simple picture of $\Delta\rho \sim AT^2 + C$ come into play, i.e. phonons and thermal smearing of the magnetic barriers.

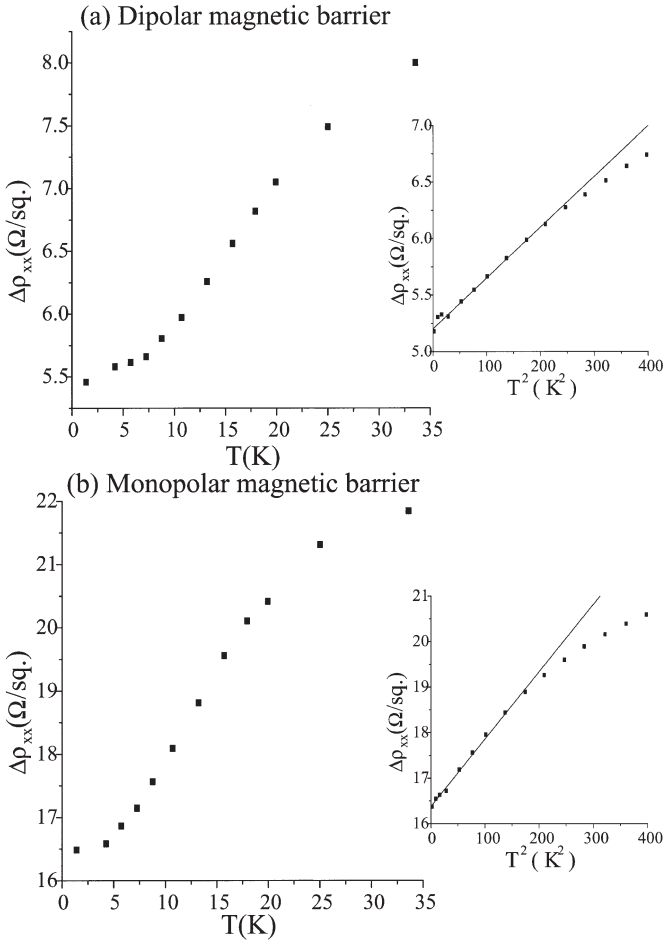

Fig. 5. Temperature dependence of the excess resistivity $\Delta\rho = \rho(\varphi = 0^\circ) - \rho(\varphi = 90^\circ)$ for the two types of magnetic barriers. The insets show the data plotted as a function of T^2.

5. Magnetoresistance

Figure 6 shows the resistivity as a function of the uniform magnetic field while the amplitude of magnetic barrier is kept constant by a strong enough parallel magnetic field. We focus on two characteristic features of these traces; positive magnetoresistance (PMR) and beating of the Shubnikov–de Haas (SdH) oscillations. The PMR is thought to be of classical origin since its temperature dependence is weak. The PMR in the dipolar barrier sample evolves in two steps. The low field PMR, which is attributed to the so-called snake orbit,[20] saturates at $\sim$0.1 T. The overall PMR curve is concave upward. By contrast, the PMR curve in the monopolar barrier sample has no low field features and is concave downward. In a semiclassical picture, the magnetoresistivity is derived from the average electron drift velocity $\langle v_d^2 \rangle$.[2]

$$\frac{\Delta\rho_{xx}}{\rho_0} \simeq \omega_c^2\tau^2 \frac{\Delta\sigma_{yy}}{\sigma_0} \simeq \omega_c^2\tau^2 \frac{\langle v_d^2 \rangle}{v_F^2/2} \quad (\omega_c\tau \gg 1), \tag{7}$$

where ρ_0 is the resistivity at zero uniform magnetic field, ω_c is the cyclotron frequency, τ is the classical scattering time, and v_F is the Fermi velocity.

In order to understand the different PMR behavior for the two types of magnetic barriers, we performed numerical

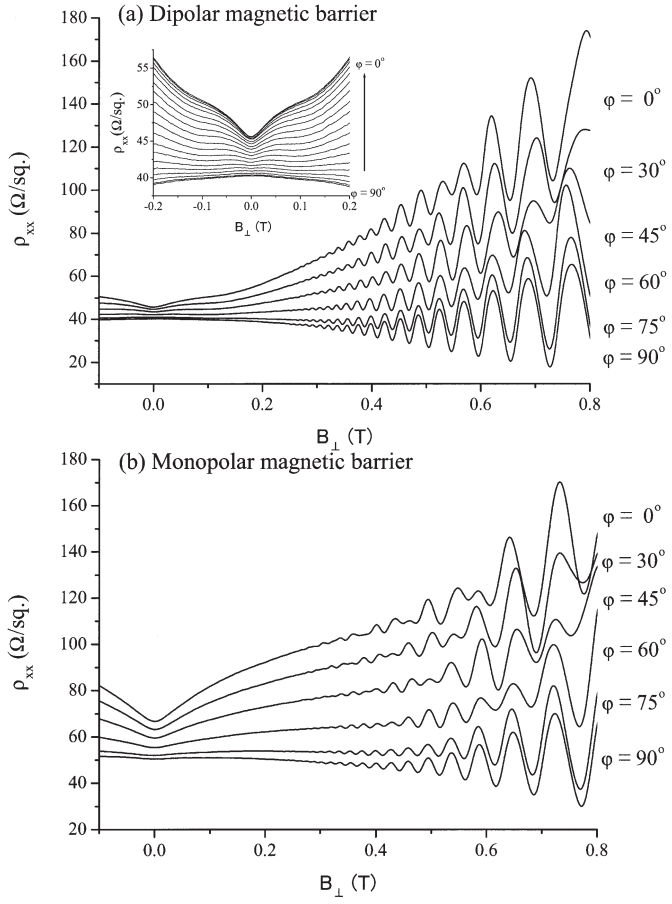

Fig. 6. Magnetoresistivity with magnetic barriers for different settings of the amplitude of magnetic barriers by changing the azimuthal angle φ of the parallel magnetic field. Inset shows the data at lower magnetic field.

calculation of electron trajectories. Figure 7 shows some representative electron trajectories in the presence of magnetic barrier and uniform magnetic field. For the ease of numerical calculation, the magnetic barriers were assumed rectangular in shape, and the amplitude was taken to be 0.15 T for the dipolar case and 0.2 T for the monopolar case, to mimic the actual situations. For the monopolar magnetic barrier, the drift motion of electrons monotonically diminishes with increasing uniform magnetic field. By contrast, for the dipolar barriers, those trajectories trapped along the center line of the barrier make significant contribution to the drift motion at higher fields. Figure 8 shows the magnetoresistivity curves numerically calculated on the basis of this semiclassical model. The sudden drop of magnetoresistivity occurring at 0.15 T (for the dipolar barrier) and at 0.2 T (for the negative monopolar barrier) corresponds to the point where the uniform field exceeds the barrier amplitude and hence the spatial region with magnetic field of wrong sign disappears. For the dipolar barrier case, the pronounced peak in the calculated curve corresponds to the inflection seen in the experimental curves around 0.1 T which is highlighted in the inset of Fig. 6(a). For the monopolar barrier case, the theoretical curve, which is given by a series-circuit sum of the two curves shown for the positive and negative barrier, is in qualitative agreement with the experimental curves.

As seen in Fig. 6, the SdH oscillations develop a beating pattern as the magnetic barrier amplitude is increased. Fourier spectra of these traces are shown in Fig. 9. They have revealed spectra consisting of a central peak (large arrow) and a side band on each side (smaller arrows). The former, which is independent of the barrier amplitude, corresponds to the cyclotron orbit in the homogeneous

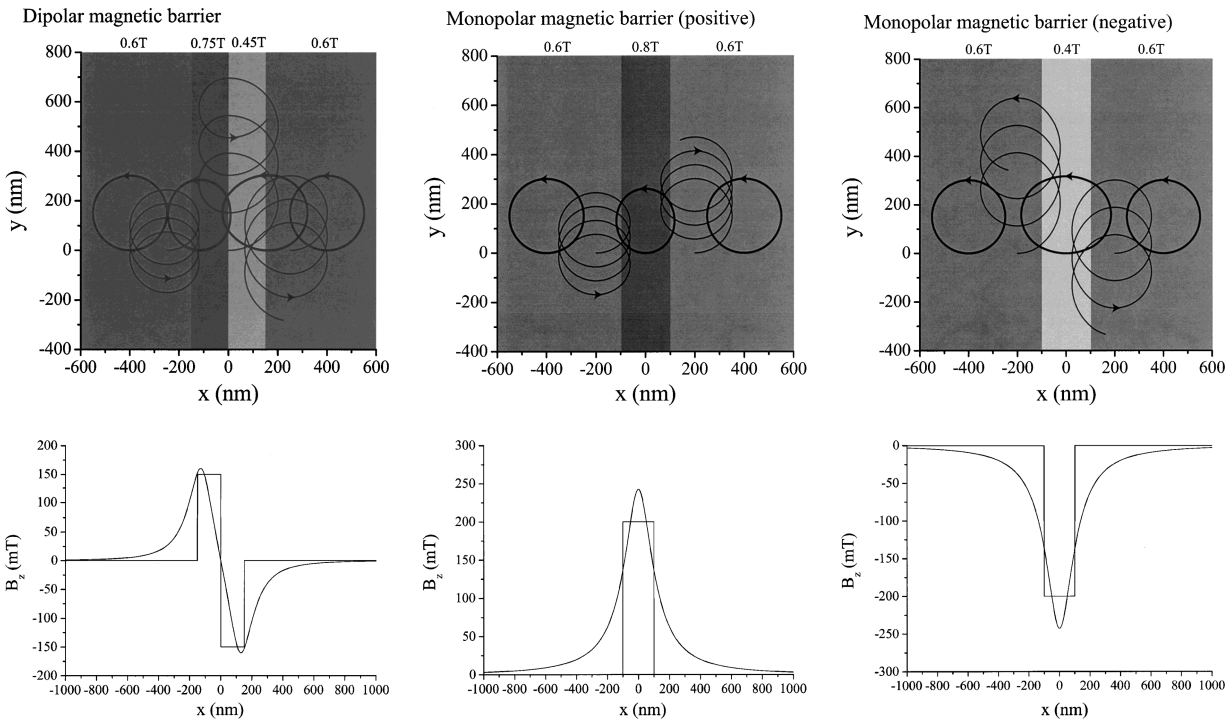

Fig. 7. Electron orbits in the presence of simplified rectangular magnetic barriers at uniform magnetic field $B_\perp = 0.6$ T. The lower graph shows calculated magnetic field profile and approximated rectangular magnetic barrier. For monopolar barrier, "positive" means that the direction of magnetic barrier is same with the uniform magnetic field, "negative" means opposite.

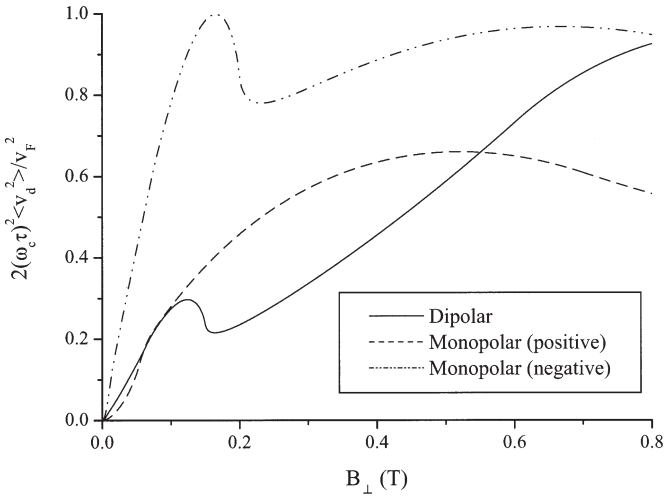

Fig. 8. Numerical calculation of the normalized magnetoresistivity in eq. (7). Drift velocity of electron $\langle v_d^2 \rangle$ was averaged out within 2.5 μm of the center of the barrier. For monopolar barrier, we observe the average of "positive" and "negative" in this experiment.

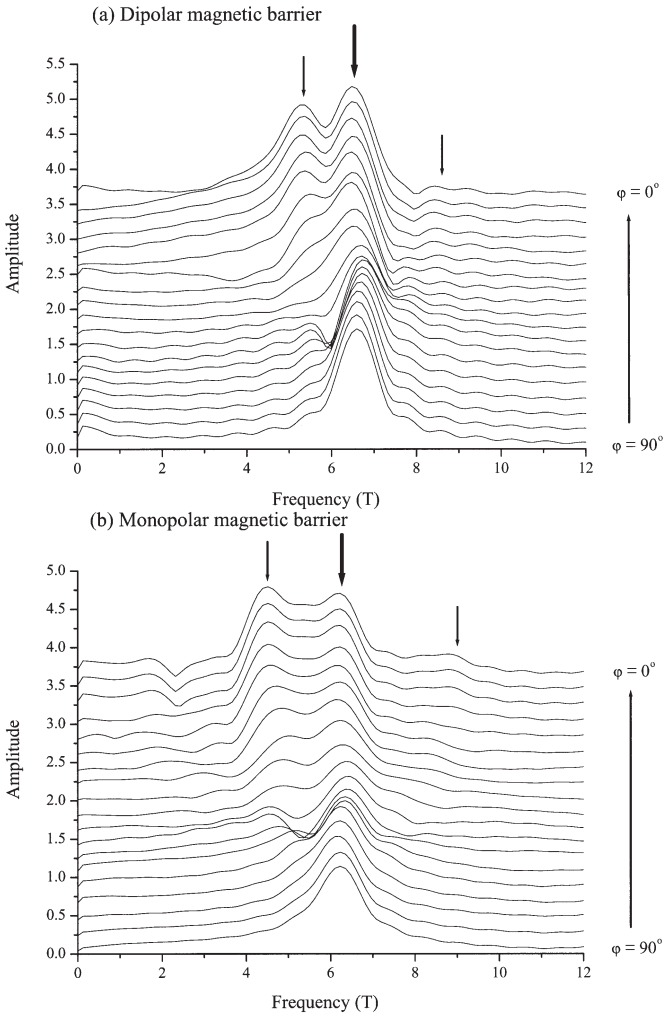

Fig. 9. Fourier spectra of beating pattern of SdH oscillations. Component of oscillations between 0.4 T and 0.8 T is Fourier transformed. The large arrow indicates the central peak which corresponds to the cyclotron orbit in the homogeneous region. The smaller arrows indicate the side band peak due to stationary trajectory in the region of magnetic barriers.

region between the barriers. The latter is attributed to the stationary trajectories shown in Fig. 6 in the region of the magnetic barriers. We can see the left side band more clearly than the right side band. It is consistent with the fact that SdH oscillations are clearly observed as increasing perpendicular magnetic field. Unlike the case of spatially varying electron density, the splitting of the SdH frequency in this case is dependent on the strength of the uniform magnetic field.

6. Conclusion

We have investigated transport in 2DEG with two different types of magnetic barrier. The excess resistivity $\Delta\rho$ due to the magnetic barriers varies as $B_0^{\nu}(\nu \sim 1.5\text{–}1.8)$ with increasing barrier amplitude. The behavior at finite temperatures, $\Delta\rho \sim AT^2 + C$, is common to two types of barrier and periodic modulation case. The positive magnetoresistance are qualitatively attributed to the drift motion under the spatially varying magnetic field. Fourier analysis of the beating pattern furnishes information on the quantum state of the stationary trajectories in the region of the magnetic barriers.

Acknowledgements

We thank T. Sasaki, H. Fukuyama, S. Uryu and T. Ando for helpful discussions. This work was supported in part by a Grant-in-Aid for COE Research (No. 12CE2004 "Control of Electronics by Quantum Dot Structures and Its Application to Advanced Electronics") and a Grant-in-Aid for Scientific Research (No. 13304025) from the Ministry of Education, Culture, Sports, Science and Technology (MEXT) Japan.

1) D. Weiss, K. von Klitzing, K. Ploog and G. Weimann: Europhys. Lett. **8** (1989) 179.
2) C. W. J. Beenakker: Phys. Rev. Lett. **62** (1989) 2020.
3) R. Yagi and Y. Iye: J. Phys. Soc. Jpn. **62** (1993) 1279.
4) D. P. Xue and G. Xiao: Phys. Rev. B **45** (1992) 5986.
5) F. M. Peeters and P. Vasilopoulos: Phys. Rev. B **47** (1993) 1466.
6) S. Izawa, S. Katsumoto, A. Endo and Y. Iye: J. Phys. Soc. Jpn. **64** (1995) 706.
7) H. A. Carmona, A. K. Geim, A. Nogaret, P. C. Main, T. J. Foster, M. Henini, S. P. Beaumont and M. G. Blamire: Phys. Rev. Lett. **74** (1995) 3009.
8) P. D. Ye, D. Weiss, R. R. Gerhardts, M. Seeger, K. von Klitzing, K. Eberl and H. Nickel: Phys. Rev. Lett. **74** (1995) 3013.
9) A. Messica, A. Soibel, U. Meirav, A. Stern, H. Shtrikman, V. Umansky and D. Mahalu: Phys. Rev. Lett. **78** (1997) 705.
10) M. Kato, A. Endo, S. Katsumoto and Y. Iye: Phys. Rev. B **58** (1998) 4876.
11) N. Overend, A. Nogaret, B. L. Gallagher, P. C. Main, R. Wirtz, R. Newbury, M. A. Howson and S. P. Beaumont: Physica B **249–251** (1998) 326.
12) V. Kubrak, A. W. Rushforth, A. C. Neumann, F. Rahman, B. L. Gallagher, P. C. Main, M. Henini, C. H. Marrows and B. J. Hickey: Physica E **7** (2000) 997.
13) E. Skuras, A. R. Long, I. A. Larkin, J. H. Davies and M. C. Holland: Appl. Phys. Lett. **70** (1997) 871.
14) In our earlier paper,[10] we reported $\Delta\rho \sim B_0^2$. But we carried out more precise measurements recently and obtained $\Delta\rho \sim B_0^{3/2}$ for the periodic case.
15) A. Matulis and F. M. Peeters: Phys. Rev. B **62** (2000) 91.
16) M. Kato, A. Endo, M. Sakairi, S. Katsumoto and Y. Iye: J. Phys. Soc. Jpn. **68** (1999) 1492.
17) M. Kato, A. Endo, S. Katsumoto and Y. Iye: J. Phys. Soc. Jpn. **68** (1999) 2870.

18) T. Sasaki and H. Fukuyama: submitted to J. Phys. Soc. Jpn.
19) S. Uryu and T. Ando: Proc. 25th Int. Conf. Physics of Semiconductors, Osaka, 2000, p. 1335.
20) A. Nogaret, S. Carlton, B. L. Gallagher, P. C. Main, M. Henini, R. Wirtz, R. Newbury, M. A. Howson and S. P. Beaumont: Phys. Rev. B **55** (1997) R16037.